

Mems-based pzt/pzt bimorph thick film vibration energy harvester

Xu, Ruichao; Lei, Anders; Dahl-Petersen, Christian; Hansen, K.; Guizzetti, M.; Birkelund, Karen; Thomsen, Erik Vilain; Hansen, Ole

Published in:

Proceedings of the International Workshops on Micro and Nanotechnology for Power Generation and Energy Conversion Applications

Publication date:
2011

Document Version
Publisher's PDF, also known as Version of record

[Link back to DTU Orbit](#)

Citation (APA):

Xu, R., Lei, A., Dahl-Petersen, C., Hansen, K., Guizzetti, M., Birkelund, K., ... Hansen, O. (2011). Mems-based pzt/pzt bimorph thick film vibration energy harvester. In Proceedings of the International Workshops on Micro and Nanotechnology for Power Generation and Energy Conversion Applications

DTU Library

Technical Information Center of Denmark

General rights

Copyright and moral rights for the publications made accessible in the public portal are retained by the authors and/or other copyright owners and it is a condition of accessing publications that users recognise and abide by the legal requirements associated with these rights.

- Users may download and print one copy of any publication from the public portal for the purpose of private study or research.
- You may not further distribute the material or use it for any profit-making activity or commercial gain
- You may freely distribute the URL identifying the publication in the public portal

If you believe that this document breaches copyright please contact us providing details, and we will remove access to the work immediately and investigate your claim.

MEMS-BASED PZT/PZT BIMORPH THICK FILM VIBRATION ENERGY HARVESTER

R. Xu¹, A. Lei¹, C. Dahl-Petersen¹, K. Hansen², M. Guizzetti², K. Birkelund¹, E.V. Thomsen¹ and O. Hansen^{1,3}

¹Department of Micro- and Nanotechnology, Technical University of Denmark, DTU Nanotech, Building 345 East, DK-2800 Kongens Lyngby, Denmark

²Meggitt Sensing Systems, DK-3490 Kvistgaard, Denmark

³CINF, Center for Individual Nanoparticle Functionality, Technical University of Denmark

*Presenting Author: ruichao.xu@nanotech.dtu.dk

Abstract: We describe fabrication and characterization of a significantly improved version of a MEMS-based PZT/PZT thick film bimorph vibration energy harvester with an integrated silicon proof mass. The main advantage of bimorph vibration energy harvesters is that strain energy is not lost in mechanical support materials since only PZT is strained, and thus it has a potential for significantly higher output power. An improved process scheme for the energy harvester resulted in a robust fabrication process with a record high fabrication yield of 98.6%. Moreover, the robust fabrication process allowed a high pressure treatment of the screen printed PZT thick films prior to sintering, improving the PZT thick film performance and harvester power output reaches 37.1 μW at 1 g.

Keywords: Energy harvesting, scavenging, piezoelectric, PZT, bimorph, thick film, MEMS, screen printing.

INTRODUCTION

One of the most severe challenges man is facing today is to fulfil the need for energy without harmful environmental consequences. This complicated, huge challenge must be met by a wide range of solutions; among these are more efficient use of resources and replacement of fossil fuels by renewable energy sources. More efficient use of resources will require more widespread use of sensing micro-systems to control and optimize processes. Some of these systems will be placed in remote areas where it is desirable if the system is self supported with power, a feature that will be equally desirable for the increasing number of portable complex electronic systems in use today.

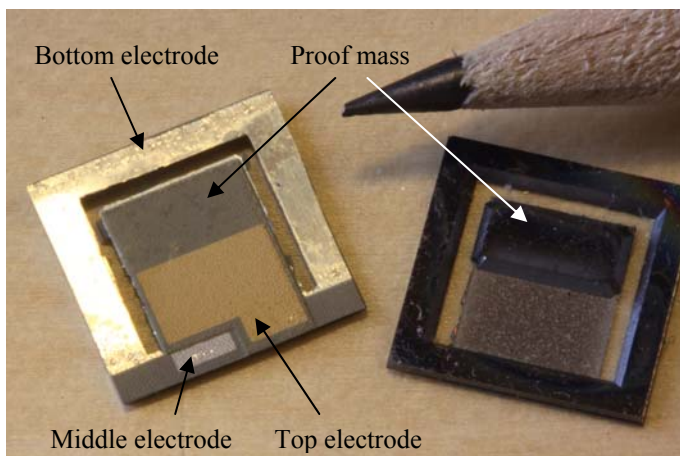


Fig. 1: Photographic image showing the front and back of the 10 mm \times 10 mm energy harvesters.

In the external surroundings energy such as ambient light, mechanical vibrations, sound, or thermal gradients is available to be harvested for free. With the advances in micro-technology many useful electronic

systems have low enough power requirements to make completely self supported systems realistic. One of the methods to harvest mechanical energy from vibrations is to make use of the piezoelectric transduction mechanism [1]. A typical piezoelectric energy harvester is based on a cantilever beam, which consists of the active piezoelectric ceramic with metal electrodes on both sides and a passive mechanical support structure, anchored at one end and with a proof mass at the other [2, 3, 4, 5]. The main advantage of PZT/PZT thick film bimorph energy harvesters, compared to the aforementioned harvesters, is that strain energy is not lost in mechanical support materials since only PZT is strained, and thus it has a potential for higher power output. The first generation bimorph PZT/PZT thick film harvester was presented in [6], where it was shown that by using PZT thick film, it is possible to realize a self supporting device without the need of a passive mechanical structure. However, the fabrication yield was low due to a process sequence with an early deep reactive ion etch (DRIE) step, which turned most of the structure into a fragile membrane. A revised process plan, using the advantageous process steps introduced in [7], has significantly improved both fabrication yield and performance of the harvesters. The DRIE step was replaced by a KOH wet etch and moved to the last part of the fabrication process; and as a result the fabrication yield was more than tripled to a record high yield of 98.6%. As an added benefit the improved mechanical stability of the structure during PZT thick film, InSensor® TF2100, deposition and processing allowed high pressure treatment of the PZT thick film before sintering, this resulted in more than a fivefold improvement of the harvester power output compared to previous results [6]. Furthermore, the use of KOH etching may facilitate a scalable future mass

production.

FABRICATION

The fabricated energy harvester, shown in Fig. 1, combines PZT thick film screen printing with standard MEMS technology.

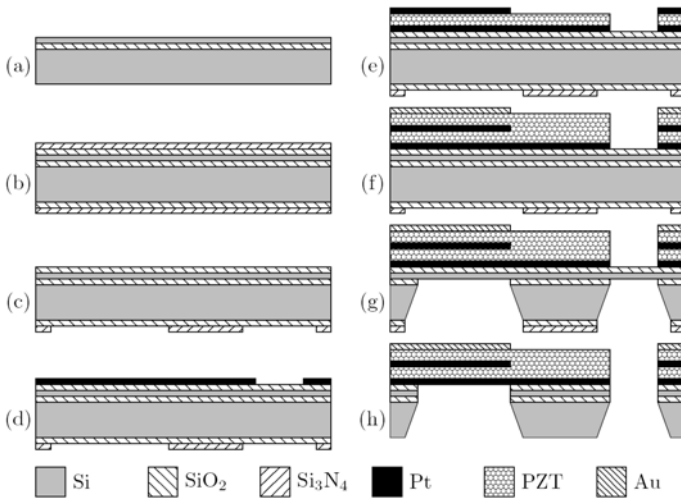


Fig. 2: Cross sectional view of the fabrication scheme.

The fabrication process is illustrated in Fig. 2. The fabrication process starts with a silicon on insulator (SOI) wafer with 20 μm device layer and 1 μm buried oxide on a 525 μm handle substrate, as shown in Fig. 2(a). First, a 1 μm thick silicon dioxide is thermally grown, and then a 170 nm thick silicon nitride is deposited using low pressure chemical vapour deposition (LPCVD), as shown in Fig. 2(b). The nitride is removed on the front side using RIE, and after that the back side of the wafer is patterned using conventional lithography processes and similarly etched in RIE, as shown in Fig. 2(c). A 50 nm Ti adhesion layer and a 500 nm Pt for the bottom electrode are deposited on the front side of the wafer, and subsequently patterned, using AZ4562 resist, followed by an etch in a wet etch solution, $\text{H}_2\text{O}:\text{HCl}:\text{HNO}_3$ (8:7:1) at elevated temperature, as shown in Fig. 2(d). Thereafter the PZT thick film layer is screen printed on the patterned bottom electrode, high pressure treated [8] and sintered, here the bottom electrode serves as a diffusion barrier. Here the advantage in the new fabrication process appears: screen printing and high pressure treatment of the PZT layer on a full wafer; instead of a wafer with thin membranes as it was done in [6], not only prevents any chip loss during this step but also ensures a higher quality thick film that will prevent any cantilever breakage after the final release etch. Next, the 500 nm Pt middle electrode is deposited through a prefabricated silicon shadow mask using e-beam evaporation, as shown in Fig. 2(e). The shadow mask was made using a 350 μm silicon wafer, which was patterned using UV lithography and etched through in a DRIE process. The second PZT thick film layer is then screen printed, high pressure treated and sintered. This is followed by deposition of a 500 nm Au top

electrode through another prefabricated shadow mask, fabricated using the aforementioned fabrication steps, see Fig. 2(f). Thereafter the wafer is mounted on a 4" tandem series wafer holder from Advanced Micromachining Tools (AMMT). The oxide on the backside is etched in buffered hydrofluoric acid (bHF), while the front side of the SOI wafer is protected by the holder. Then the silicon is etched in a KOH etch until the buried oxide layer is reached and then the buried oxide layer is removed in bHF, as shown in Fig. 2(g). Finally, the sacrificial device layer is etched in RIE, releasing the cantilevers; see Fig. 2(h).

Figure 3 shows the fabricated harvester wafer before dicing. Notice that all cantilevers are intact, the chip yield on the wafer at this stage is still 100%, while if the fabrication process from [6] was used the chip yield would be much less.

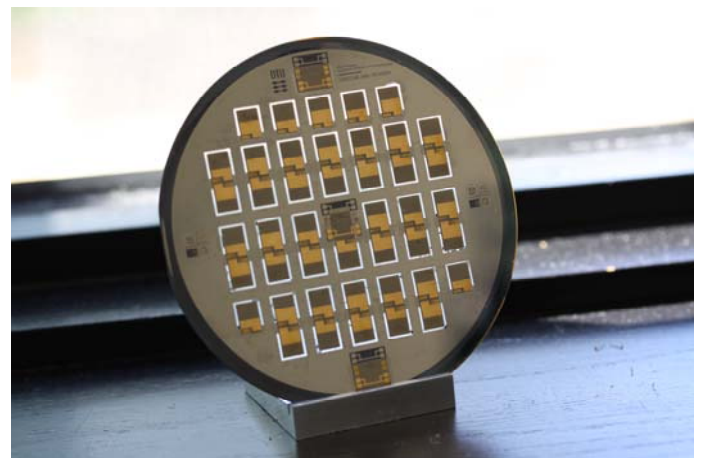


Fig. 3: Image of a fabricated harvester wafer before dicing.

The wafer is diced and the chips polarized individually. The polarization directions of the two layers are aligned opposite to each other, *i.e.* during polarization the top and bottom electrodes are grounded and a polarization voltage is applied to the middle electrode. The dimensions for the final energy harvester chips are shown in Table 1.

Table 1: Energy harvester dimensions.

Frame dimensions	10 mm \times 10 mm
Medial dimensions	< 1 mm
Cantilever width	5.5 mm
Cantilever length	3.25 mm
Mass length	3.25 mm
Total cantilever height	2 \times 20 μm

RESULTS

The fabricated energy harvesters were characterized in a shaker setup, where a B&K Mini Shaker 4810 driven by an amplified sinusoidal signal from an Agilent 33220A function generator was used to simulate an external vibration from the environment. Both the energy harvester and a B&K Piezoelectric Accelerometer 8305 were mounted on

the Mini Shaker. The accelerometer served as a reference for the input RMS acceleration and measurements are reported in fractions of the gravitational acceleration g (9.81 m s^{-2}). The RMS power output is found by connecting the harvester to a resistive load while the voltage drop across the load was measured. The optimal resistive load, R_{opt} , was found by varying the resistive load in steps of $10 \text{ k}\Omega$ to achieve maximum dissipated power in the load resistance, *i.e.* $P_{\text{RMS}}=V_{\text{RMS}}^2/R_{\text{opt}}$. Figure 4 shows the power output of the harvester as a function of the frequency for different input accelerations, measured with the PZT layers connected in series, *i.e.* the load is connected between bottom and top electrodes. The optimal resistive load used here was $R_{\text{opt}}=200 \text{ k}\Omega$. At 1 g input acceleration the power output reaches $37.1 \mu\text{W}$.

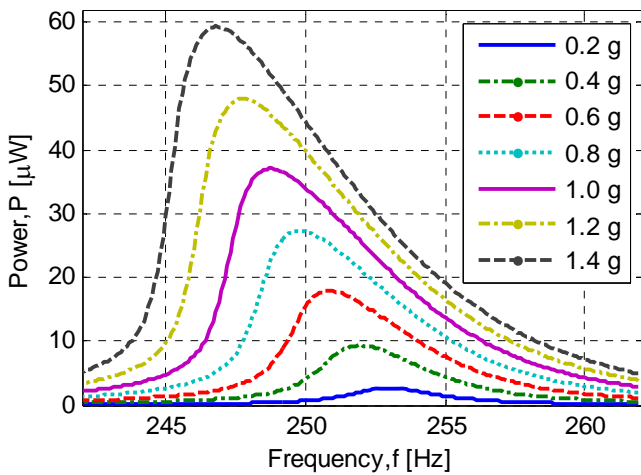


Fig. 4: RMS power output of both PZT layers combined as a function of frequency near the resonant frequency for different input accelerations at an optimal resistive load of $200 \text{ k}\Omega$

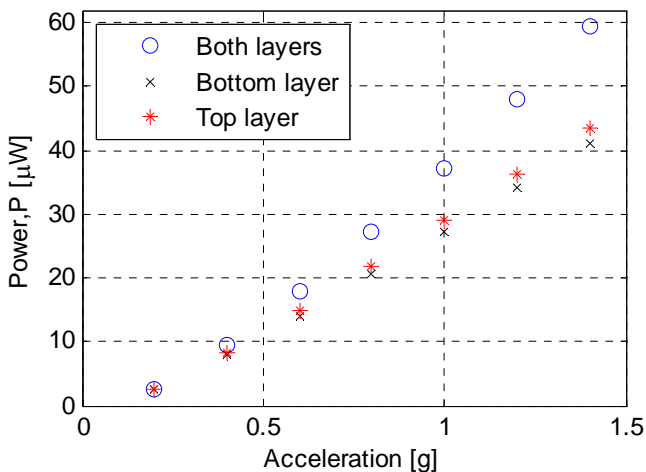


Fig. 5: RMS power output from the top PZT layer, the bottom PZT layer and both layers combined as a function of the input acceleration at their respective optimal resistive loads.

The output power from the bottom PZT layer and the top PZT layer were measured using the same

measurement scheme. During measurements on the top PZT layer, the top and middle electrodes were connected while the bottom electrode was left open circuit. The optimal resistive load was found to be $130 \text{ k}\Omega$ for the top layer. Similarly, during measurements on the bottom PZT layer the bottom and middle electrodes were connected and the top electrode was left open circuit. The optimal resistive load was found to be $90 \text{ k}\Omega$ for the bottom layer. Collecting the peak output power from the measurements yields the plot reported in Fig. 5, where the output power is shown as a function of the input acceleration. The bandwidth, defined as the full width at half maximum of the data such as those in Fig. 4, was extracted for all measurements and it is reported in Fig. 6.

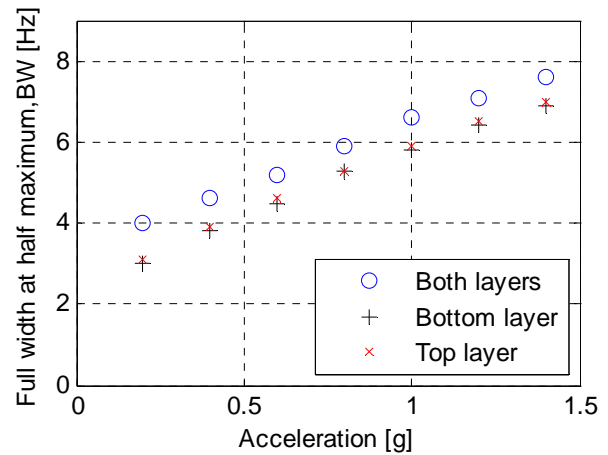


Fig. 6: The full width at half maximum bandwidth for the top PZT layer, the bottom PZT layer and both layers combined as a function of the input acceleration at their respective optimal resistive loads.

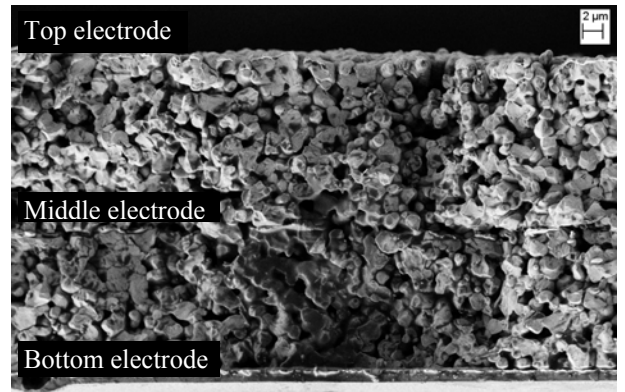


Fig. 7: SEM image showing a cross-sectional view of the PZT/PZT bimorph thick film structure.

DISCUSSION

The resonant frequency shift as a function of the acceleration observed in Fig. 4 was also seen in [6], where it was assumed to be due to a non linear softening effect. Even though such an effect is still present in the pressure treated harvester, the softening effect is much less prominent compared to that in [6].

As a result, the resonant frequency shift with acceleration is smaller, and the frequency responses become more symmetrical around the resonance peaks.

From Fig. 5 it can be noted that the power outputs of the two individual layers are almost identical, this was not the case in [6]. Apparently, the use of high pressure treatments renders the PZT thick film layers quite similar. This is supported by the SEM inspection shown in Fig. 7, where a cross sectional view of the cantilever shows that the two layers are very similar both in thickness and morphology which was not the case in a similar study in [6]. The difference in the optimal resistive loads with such similar films is surprising and thus still needs further investigation. The output power from both layers combined in series is less than the sum of the powers from the two individual layers. This, to some extent, may be explained by Fig. 6, where the bandwidth of both layers combined in series is about 1 Hz larger than that of each layer for all input accelerations. As a result the output power is not doubled by the use of two PZT layers, but it is still increased significantly; moreover, the harvester becomes useful in a wider spectrum of vibrations due to the increase in bandwidth. The measured RMS power output at 1 g acceleration is 37.1 μW , which is comparable to the best performing MEMS energy harvesters reported in literature in recent years [5, 9].

CONCLUSION

MEMS-based PZT/PZT bimorph thick film vibration energy harvesters were successfully fabricated and characterized. By implementing an improved fabrication process a fabrication yield of 98.6% was achieved. The revised process plan made high pressure treatment of the PZT thick film layers before sintering feasible. As a result the two PZT layers became denser and more similar in thickness and morphology. The power outputs at 1 g for the top and bottom layers were 29.1 μW and 27.2 μW , respectively. The power output with both layers combined was 37.1 μW at 1 g with a bandwidth value of 7 Hz.

REFERENCES

- [1] Beeby S P, Tudor M J, White N M, 2006 Energy harvesting vibration sources for Microsystems applications *Measurement Science and Technology* **17** no. 12, R175-R195
- [2] Fang H, Liu J, Xu Z, Dong L, Wang L, Chen D, Cai B, Liu Y, 2006 Fabrication and performance of MEMS-based piezoelectric power generator for vibration energy harvesting *Microelectronics Journal* **37** 1280-1284.
- [3] Choi W J, Jeon Y, Jeong J H, Sood R, Kim S G 2006 Energy harvesting MEMS device based on thin film piezoelectric cantilevers *Journal of Electroceramics* **17** 543-548
- [4] Shen D, Park J, Ajitsaria J, Choe S, Wikle H C, Kim D, 2008 The design, fabrication and evaluation of a MEMS PZT cantilever with an integrated Si proof mass for vibration energy harvesting *Journal of Micromechanics and Microengineering* **18** no. 15 055017
- [5] Aktakka E E, Peterson R L, Najafi K, 2011 Thinned-PZT on SOI process and design optimization for piezoelectric inertial energy harvesting *Proceeding, Transducers 2011* (Beijing, China Jun 2011) 1649-1652
- [6] Xu R, Lei A, Christiansen T L, Hansen K, Guizzetti M, Birkelund K, Thomsen E V, Hansen O, 2011 Screen printed PZT/PZT thick film bimorph MEMS cantilever device for vibration energy harvesting *Proceeding, Transducers 2011* (Beijing, China Jun 2011) 679-682
- [7] Lei A, Xu R, Thyssen A, Stoot A C, Christiansen T L, Hansen K, Lou-Moeller R, Thomsen E V, Birkelund K, 2011 MEMS-Based Thick Film PZT Vibrational Energy Harvester *Proceeding, IEEE micro electro mechanical systems 2011* (Cancun, Mexico January 2011) 125-128
- [8] Hindrichsen C, Lou-Moeller R, Hansen K, and Thomsen E V, 2010 Advantages of PZT thick film for MEMS sensors *Sensors and Actuators A: Physical* **163** no. 1, 9 - 14
- [9] Elfrink R, Kamel T M, Goedbloed M, Matova S, Hohlfeld D, van Andel Y, van Schaijk R, 2009 Vibration energy harvesting with aluminum nitride-based piezoelectric devices *Journal of Micromechanics and Microengineering* **19** 094005